

DAMA/LIBRA and dark matter: decisive tension or contrived cancellation

Giorgio Busoni,^{1,*} Jonathan M. Cornell,^{2,†} Will Handley,^{3,‡} Felix Kahlhoefer,^{4,§} Anders Kvellestad,^{5,¶} Masen Pitts,² Lauren Street,⁶ Aaron C. Vincent,^{7,8,9,**} and Martin White^{1,††}

¹*ARC Centre of Excellence for Dark Matter Particle Physics & CSSM,
Department of Physics, University of Adelaide, Adelaide, SA 5005*

²*Department of Physics and Astronomy, Weber State University,
1415 Edvalson St., Dept. 2508, Ogden, UT 84408, USA*

³*Cavendish Laboratory, University of Cambridge,
JJ Thomson Avenue, Cambridge, CB3 0HE, UK*

⁴*Institute for Astroparticle Physics (IAP), Karlsruhe Institute of Technology (KIT),
Hermann-von-Helmholtz-Platz 1, D-76344 Eggenstein-Leopoldshafen, Germany*

⁵*Department of Physics, University of Oslo, N-0316 Oslo, Norway*

⁶*Department of Physics, University of Cincinnati, Cincinnati, OH 45221, USA*

⁷*Department of Physics, Engineering Physics and Astronomy,
Queen's University, Kingston ON K7L 3N6, Canada*

⁸*Arthur B. McDonald Canadian Astroparticle Physics Research Institute, Kingston ON K7L 3N6, Canada*

⁹*Perimeter Institute for Theoretical Physics, Waterloo ON N2L 2Y5, Canada*

We assess the tension between DAMA/LIBRA and the latest dark matter annual modulation results from the ANAIS-112 and COSINE-100 NaI experiments, under a range of hypotheses ranging from physical to general parameterisations. We find that, in the most physically-motivated cases, the tension between DAMA and these other NaI experiments exceeds 5σ . Lowering the tension to reasonable values requires significant tuning, such as overfitting with large numbers of free parameters, and opposite-sign modulation between recoil signals on sodium versus iodine.

Introduction—It has been over two decades since the DAMA/LIBRA NaI experiment claimed the discovery of an annual modulation signal of dark matter (DM) at 6.3σ [1]. In combination with DAMA/LIBRA and DAMA/LIBRA phase2, 2.86 ton-yr of exposure over 22 annual cycles have now yielded a claimed signal over 13σ [2]. Multiple analyses have shown that the energy dependence of this signal leads to a preference for a particle with a mass around 10 or 50 GeV, depending on whether it scatters primarily off sodium or iodine (e.g. [3, 4]). In parallel, however, advances in large direct detection experiments such as SuperCDMS, PICO-60, LZ and XENON1T have left very little room for a DM interpretation, with the current sensitivity being a full six orders of magnitude below DAMA/LIBRA’s region of interest [5–10]. Nonetheless, the DAMA/LIBRA DM interpretation has persisted on the premise that no experiment to date has formally excluded it by searching for an annual modulation signature with the same technology, namely extremely pure NaI scintillator crystals, leaving the door open to DM particles with some inscrutable affinity towards sodium or iodine. While some exploratory efforts occurred starting from the early 2000s [11–13], none of these experiments were able to completely exclude DAMA/LIBRA in a model-agnostic way.

In recent years, a new generation of NaI experiments has been releasing data: the ANAIS-112 detector [14–17], located in Canfranc and COSINE-100 [18–22], at Yangyang. Neither of these experiments alone has quite reached the 5σ sensitivity to conclusively rule out the NaI-philic DM hypothesis of DAMA/LIBRA. A recent joint analysis [23] combining these datasets into two single-energy bins has excluded a modulation signal compatible with DAMA’s at the level of 4.68σ (3.53σ) in the 1–6 (2–6) keV range.

In addition, the two experiments have separately determined modulation amplitudes for events binned in energy [17, 22], assuming the expected phase for DM scattering, a useful result for model discrimination. These can be directly compared to similar results previously reported by DAMA [24]. Performing such a comparison will be the goal of this letter. We use the full spectral information reported by the different experiments and determine how well we can reconcile the spectra reported by DAMA/LIBRA and COSINE-100/ANAIS-112 if we assume the modulation is due to DM-nucleon scattering. This comparison is not as trivial as it may seem: given a common *nuclear recoil spectrum*, the differences in binning and energy resolution can lead to substantially different predictions for the *measured* modulation spectrum between the various experiments. To remain as general as possible, we adopt two different model-independent approaches: a DM effective field theory in which the nuclear recoil spectrum is calculable and a more general scenario where the nuclear recoil spectrum is parameterized with various functional forms. We undertake fits to the experimental data sets to determine the best-fit parameters of these models, and based on these results we

* giorgio.busoni@adelaide.edu.au

† jonathancornell@weber.edu

‡ wh260@cam.ac.uk

§ kahlhoefer@kit.edu

¶ anders.kvellestad@fys.uio.no

** aaron.vincent@queensu.ca

†† martin.white@adelaide.edu.au

quantify the tension between the experiments.

Background— The scattering rate of weakly-interacting DM particles from a nuclear target is given in terms of the differential cross section $d\sigma/dE_R$ by

$$\frac{dR}{dE_R} = \frac{\rho_0}{m_\chi m_N} \int_{v_{\min}}^{v_{\max}} d^3v v \tilde{f}(\mathbf{v}, t) \frac{d\sigma}{dE_R} \quad (1)$$

where ρ_0 is the local DM mass density, m_χ is the DM particle mass, m_N is the mass of the recoiling nucleus, v_{\max} is the escape velocity and v_{\min} is the minimum velocity needed to cause a nucleus to recoil with energy E_R . $\tilde{f}(\mathbf{v}, t)$ is the DM velocity distribution in the lab frame. The lab-frame distribution is related to the Galactic frame distribution $f(\mathbf{v})$ by a Galilean boost: $\tilde{f}(\mathbf{v}) = f(\mathbf{v} + \mathbf{v}_{\text{obs}}(t))$, where $\mathbf{v}_{\text{obs}}(t) = \mathbf{v}_\odot + \mathbf{V}_\oplus(t)$, \mathbf{v}_\odot is the velocity of the Sun relative to the DM reference frame and \mathbf{V}_\oplus is the velocity of the Earth about the Sun. In Boreal summer, the addition of the Earth’s orbital velocity with that of the Sun boosts the “wind” of DM in our rest frame, whilst the wind is slower during the Austral summer. This changes the number of particles above the minimum speed required to create an observable nuclear recoil. The resulting annual modulation [25–27] is parameterised as

$$\frac{dR}{dE_R} = A_0 + A_1 \cos[\omega(t - t_0)] + \dots \quad (2)$$

Experimental results are reported not in terms of the nuclear recoil energy E_R but in terms of the measured electron-equivalent energy E_{ee} , which is related to the former by a quenching factor $Q_T(E_R)$ that depends on both the target T and the recoil energy. For a NaI detector with two potential nuclear targets $T = \{\text{Na}, \text{I}\}$, the total number of events in a given experimental bin i is given by

$$N_i = \int_{E_{i,\min}}^{E_{i,\max}} dE_{ee} \epsilon(E_{ee}) \times \int_0^\infty dE_R \sum_T \xi_T \frac{1}{\sqrt{2\pi}\sigma(E_{ee})} e^{-\frac{(E_{ee} - Q_T(E_R)E_R)^2}{2\sigma(E_{ee})^2}} \frac{dR_T}{dE_R}, \quad (3)$$

where ξ_T indicates the mass fraction of the target T , dR_T/dE_R is the predicted recoil energy spectrum for that target, $E_{i,\min}, E_{i,\max}$ define the bin energy range, ϵ is the detector efficiency and σ is the detector resolution. As all collaborations report efficiency-corrected results, we will set $\epsilon = 1$ for all detectors.

DAMA/LIBRA phases 1 and 2 [24, 28] have reported results compatible with a DM annual modulation signature in the energy range 1 – 6 keV_{ee}. However, they have presented results over a larger energy range, with DAMA/LIBRA-phase2 releasing data in the energy range 0.75 – 20 keV_{ee} with a total exposure over 8 annual cycles of 1.53 t×yr. This is in addition to data from DAMA/NaI and DAMA/LIBRA-phase1, which bring the total exposure in the range 2 – 20 keV_{ee} to 2.86 t×yr.

In this work we fit to all of the available modulation data as presented in [24]. The DAMA/LIBRA detector resolution is taken to be $\sigma(E_{ee}) = a\sqrt{E_{ee}} + bE_{ee}$ with $a = 0.488\sqrt{\text{keV}_{ee}}$ and $b = 0.0091$ [29].

COSINE-100 recently released results with 6.4yr of exposure [22], where they find no evidence of an annual modulation signal and a greater than 3σ tension with DAMA/LIBRA in the energy range 1 – 6 keV_{ee}. In our fits, we include their reported modulations in the range 0.75 – 20 keV_{ee} and make use of the detector resolution presented in [30]: $\sigma(E_{ee}) = \sqrt{aE_{ee} + bE_{ee}^2}$ with $a = 0.081483 \text{ keV}_{ee}$, $b = 0.001885$.

ANAIS-112 recently presented binned modulation amplitude data from their 6-year exposure dataset [17]. This data is incompatible with the DAMA/LIBRA modulation signal in the 1–6 keV_{ee} range at nearly 4σ confidence level. We fit to their reported modulation amplitudes over the range 1 – 20 keV_{ee}, and take the detector resolution to be $\sigma(E_{ee}) = a + b\sqrt{E_{ee}}$ with $a = -0.08 \text{ keV}_{ee}$, $b = 0.378\sqrt{\text{keV}_{ee}}$ [31].

Equally important is the nuclear recoil quenching factor $Q_T(E_R)$, defined as the ratio of scintillation light yield produced by nuclear recoil to that of electron recoil at the same energy. We take recently-measured energy-dependent quenching factors for sodium from Ref. [22] and iodine from Ref. [32], for all experiments. We will, however, examine the impact of alternative quenching factors.

Quantifying the tension between the datasets—

We follow the approach from [33] to quantify the tension between the datasets of different experiments.

Consider two experiments, A and B , that measure a number of observables m_A and m_B , respectively, and a model that describes the signal using n parameters c_i . We define $\chi_X^2(c_i)$ as the χ^2 obtained from the data of experiment $X = A, B$. We denote the best-fit point obtained by fitting the data of experiment X alone as c_i^X , so that $\chi_X^2(c_i)$ has a minimum at $c_i = c_i^X$. Similarly, c_i^{A+B} is the best-fit point obtained by fitting the data of both experiments simultaneously. In this case, the function

$$\chi_{A+B}^2(c_i) = \chi_A^2(c_i) + \chi_B^2(c_i) \quad (4)$$

has a minimum at $c_i = c_i^{A+B}$, and the quantity

$$\delta\chi^2 = \chi_{A+B}^2(c_i^{A+B}) - \chi_A^2(c_i^A) - \chi_B^2(c_i^B) \quad (5)$$

follows a χ^2 distribution with n degrees of freedom.

This can be used to determine the level of statistical inconsistency of the two datasets, under the assumption that the chosen model describes the signals with the right level of precision to reproduce the data of the experiments. We will use this statistical test to assess the compatibility between DAMA/LIBRA and the combination of COSINE-100 and ANAIS-112. We will employ two qualitatively different approaches to derive the tension between the DAMA/LIBRA and combined COSINE-100 and ANAIS-112 datasets.

Detailed particle astrophysics test— The first is to use concrete assumptions for the astrophysics and particle physics defined in Eq. (1). The DM distribution $f(\mathbf{v})$, is well-described by a Maxwellian velocity distribution in the halo frame, with a peak velocity $v_0 = 240 \pm 8 \text{ km s}^{-1}$ [34], cut off at the escape velocity $v_{\text{esc}} = 528 \pm 25 \text{ km s}^{-1}$, based on *Gaia* data [35]. The halo parameters are fixed to their central values, as varying these parameters is expected to affect all experiments in the same way. The potential impact of varying the velocity distribution will be implicitly captured by the more-model-independent parametrization discussed later. On the particle physics side, we consider elastic scattering of DM on nuclei. However, instead of simply considering spin-independent and spin-dependent scattering, we adopt a more model-agnostic approach by considering an effective field theory (EFT) allowing for different types of interactions between DM and Standard Model particles. This approach avoids the need to specify the detailed microphysics of DM interactions, as long as the relevant energy scale is below the cutoff scale Λ . For elastic scattering, we can simply set Λ equal to the hadronic scale, i.e. $\Lambda = 2 \text{ GeV}$ without loss of generality.

To construct the EFT, we further assume that the DM particle is a Dirac fermion and a singlet under the Standard Model gauge group. Following the notation of Refs. [36, 37], we write the interaction Lagrangian for the theory as

$$\mathcal{L}_{\text{int}} = \sum_{a,d} \frac{C_a^{(d)}}{\Lambda^{d-4}} \mathcal{Q}_a^{(d)}, \quad (6)$$

where $\mathcal{Q}_a^{(d)}$ is a particular effective operator involving DM and Standard Model fields, $d \geq 5$ is the mass dimension of the operator and $C_a^{(d)}$ is the dimensionless Wilson coefficient associated to $\mathcal{Q}_a^{(d)}$. The full Lagrangian density for the theory is then $\mathcal{L} = \mathcal{L}_{\text{SM}} + \mathcal{L}_{\text{int}} + \bar{\chi}(i\not{\partial} - m_\chi)\chi$, such that the free parameters of the theory are the DM mass m_χ , and the set of dimensionless Wilson coefficients $\{C_a^{(d)}\}$.

The phenomenology of DM in this model will be dominated by the lowest dimension operators. We thus limit ourselves to operators with $d \leq 6$. At dimension 5, there are the two dipole operators

$$\mathcal{Q}_1^{(5)} = \frac{e}{8\pi^2} (\bar{\chi} \sigma_{\mu\nu} \chi) F^{\mu\nu}, \quad (7)$$

$$\mathcal{Q}_2^{(5)} = \frac{e}{8\pi^2} (\bar{\chi} i \sigma_{\mu\nu} \gamma_5 \chi) F^{\mu\nu}, \quad (8)$$

where $F_{\mu\nu}$ is the electromagnetic field strength tensor and e is the electromagnetic charge. These operators give rise to long-range interactions, i.e. steeply-falling recoil spectra.

At dimension six, we consider the operators

$$\mathcal{Q}_{1,q}^{(6)} = (\bar{\chi} \gamma_\mu \chi) (\bar{q} \gamma^\mu q), \quad (9)$$

$$\mathcal{Q}_{2,q}^{(6)} = (\bar{\chi} \gamma_\mu \gamma_5 \chi) (\bar{q} \gamma^\mu q), \quad (10)$$

$$\mathcal{Q}_{3,q}^{(6)} = (\bar{\chi} \gamma_\mu \chi) (\bar{q} \gamma^\mu \gamma_5 q), \quad (11)$$

$$\mathcal{Q}_{4,q}^{(6)} = (\bar{\chi} \gamma_\mu \gamma_5 \chi) (\bar{q} \gamma^\mu \gamma_5 q). \quad (12)$$

The first two operators give rise to spin-independent interactions, while the last two give rise to spin-dependent interactions. Moreover, $\mathcal{Q}_{1,q}^{(6)}$ and $\mathcal{Q}_{4,q}^{(6)}$ are independent of the momentum transfer and the DM velocity, while $\mathcal{Q}_{2,q}^{(6)}$ and $\mathcal{Q}_{3,q}^{(6)}$ vanish in the non-relativistic limit. Together these operators therefore capture a wide range of different possibilities for elastic scattering.

The effective operators are defined at the scale $\Lambda = 2 \text{ GeV}$, where the Higgs, W and Z bosons as well as the top, bottom and charm quarks have been integrated out. We do not consider interactions with leptons, which do not give rise to nuclear scattering at tree-level. Following the assumption of Minimal Flavour Violation, we take the Wilson coefficients for operators involving the down and strange quarks to be equal, but we allow the Wilson coefficients for operators involving up quarks to differ. We parameterize the relative couplings between the u and d -type quarks by angles $\theta_a^{(6)}$, in the following form:

$$C_{a,d}^{(6)} = C_a^{(6)} \sin \theta_a^{(6)} = C_{a,s}^{(6)}, \quad (13)$$

$$C_{a,u}^{(6)} = C_a^{(6)} \cos \theta_a^{(6)}. \quad (14)$$

In the EFT setup, we therefore have 11 model parameters to consider.

The fits are performed with GAMBIT [38, 39] and its DarkBit [40] module, using Diver 1.3¹ [41] to explore the parameter space, DirectDM [36, 42, 43] to match the effective operators introduced above onto the non-relativistic operators relevant for nuclear scattering, and DDCalc² [44] to evaluate nuclear form factors, calculate the differential event rate, and evaluate the experimental likelihoods.

The best-fit values for all parameters for each scan to the modulation spectrum from DAMA/LIBRA, both ANAIS-112 and COSINE-100, or all three experiments combined, are shown in Table I. The corresponding χ^2 values and resulting tension is shown in Table II. The combination of ANAIS-112 and COSINE-100 is found to rule out the DM nuclear recoil interpretation of the DAMA signal with a significance of 5.1σ .

Our best fit to the DAMA data alone prefers interactions via the $C_3^{(6)}$ operator, which induces spin- and

¹ <https://github.com/diveropt/Diver/releases/tag/v1.3.0>

² The rate calculations and likelihoods for the modulation experiments included in this paper will be part of the the upcoming DDCalc 3.0 public release.

TABLE I. EFT Parameter values that maximize individual experimental likelihoods and the likelihood for all experiments combined.

	All	DAMA	ANAIS+COSINE
m_χ [GeV]	17.1	184	102
$C_1^{(5)}$	1.41×10^{-4}	1.47×10^{-6}	2.44×10^{-5}
$C_2^{(5)}$	1.00×10^{-8}	1.04×10^{-8}	1.22×10^{-8}
$C_1^{(6)}$	6.12×10^{-5}	9.08×10^{-7}	1.51×10^{-6}
$C_2^{(6)}$	1.19×10^{-7}	8.18×10^{-4}	2.82×10^{-8}
$C_3^{(6)}$	1.47×10^{-7}	0.436	4.77×10^{-7}
$C_4^{(6)}$	3.75×10^{-7}	1.13×10^{-8}	5.37×10^{-8}
$\theta_1^{(6)}$	1.77π	0.0353π	0.676π
$\theta_2^{(6)}$	1.61π	0.482π	0.489π
$\theta_3^{(6)}$	1.89π	1.30π	1.27π
$\theta_4^{(6)}$	1.65π	0.367π	1.21π

momentum-dependent interactions, with a DM mass of 184 GeV. We find an almost equally good fit at a mass of approximately 40 GeV. Fitting to ANAIS+COSINE, as well as to all three experiments, yields small couplings to all operators, i.e. no DM signal.

Restricting the nuclear recoil energy range in DAMA below 7 keV_{ee} provides a best fit mass of 36 GeV. However, this restriction does not change the qualitative conclusions regarding the tension between DAMA and other experiments, which remains above 5σ , hence we choose to present the fit over the full range for completeness.

It has been speculated that quenching factors may be specific to individual crystals, rather than to the material itself. Since DAMA has never measured the energy dependence of its crystal’s quenching factor, they assume a constant value of 0.3 for sodium and 0.09 for iodine [45]. Measurements from other groups have consistently shown a strong energy-dependence, with sodium quenching factors never being higher than ~ 0.2 , and going as low as 0.1 below 5 keV [22]. Nonetheless, we have repeated all scans using the DAMA quenching factors for the DAMA response modeling, and still find that this only modestly reduces the tension to 4.63σ . The final column of table II shows the resulting χ^2 values.

Fig. 1 shows the expected spectrum seen at DAMA/LIBRA (left), ANAIS-112 (centre) and COSINE-100 (right), if the signal is fit to that experiment only (orange), or to all three simultaneously (red). The large discrepancy between the data points (black) and the red curves for all three experiments illustrates the tension—in this EFT model, the strong preference of DAMA for modulation at low energies leads to similar predictions for the other experiments, a scenario which the data do not support.

How generic is the tension?— The use of specific particle physics and astrophysics assumptions means that any derived tension between DAMA/LIBRA and other experiments is necessarily model-dependent. We therefore also adopt a second approach which simply replaces

TABLE II. Best fit χ^2 values for individual and combined experiments, as well as tension parameters. The first column shows the tension when all three experiments assume measured quenching factors for I and Na. The second column allows DAMA to use constant quenching factors.

	Common quenching	Different quenching for DAMA
All	181.36	173.37
DAMA/LIBRA	74.02	71.83
ANAIS+COSINE	55.85	55.85
$\delta\chi^2$	51.49	45.69
p-value	3.37×10^{-7}	3.66×10^{-6}
Tension	5.10σ	4.63σ

the right-hand side of Equation 1 by a generic functional form that is not constrained by any known particle, nuclear or astrophysics. We consider two sets of model-independent parameterisations: 1) A modulated nuclear recoil signal injected in $2N$ uniform E_R bins between 1 and 80 keV³ allowing independent bin amplitudes between recoils with sodium and iodine, and 2) a polynomial \times exponential parameterisation, inspired by the expected DM signal, but leaving coefficients completely free:

$$A_1 = \sum_{T=\text{Na,I}} (c_0^T + c_1^T E_R + c_2^T E_R^2 + \dots) e^{-d_T E_R}, \quad (15)$$

where d_T and the c_i^T are free parameters. We use Diver 1.3 embedded in GAMBIT-light⁴ to maximise the likelihoods of the resulting spectra with respect to the DAMA/LIBRA data, combined ANAIS-112 and COSINE-100 datasets, and the combination of all three experiments, and compute the tension statistic as in Eq. (5). Demanding that the spectra be produced only by scattering with Na or I further worsens the tension in all cases. Resulting best fit χ^2 values, p-values, and tension statistics are presented in the appendix.

Using the tension statistic defined above, more than 12 bins (6 Na, 6 I) are required for the tension between DAMA/LIBRA and ANAIS-112 and COSINE-100 to fall below 5σ . With 20 bins, the tension reduces to 2σ . If we only allow for a signal in Na or I, the tension does not fall below 5σ for 10 or fewer bins. Indeed, we find that the tension is only reduced when the contributions from Na and I in each bin have opposite signs (such that the one contribution peaks in summer, while the other peaks in winter), allowing for delicate cancellations to simultaneously fit the overall signal shape in all experiments

³ This range in nuclear recoil energy ensures that for quenching factors ranging from 5% to 30%, we cover the signal range in electron-equivalent energy.

⁴ GAMBIT-light is a lightweight version of GAMBIT, available at github.com/GambitBSM/gambit_light_1.0.

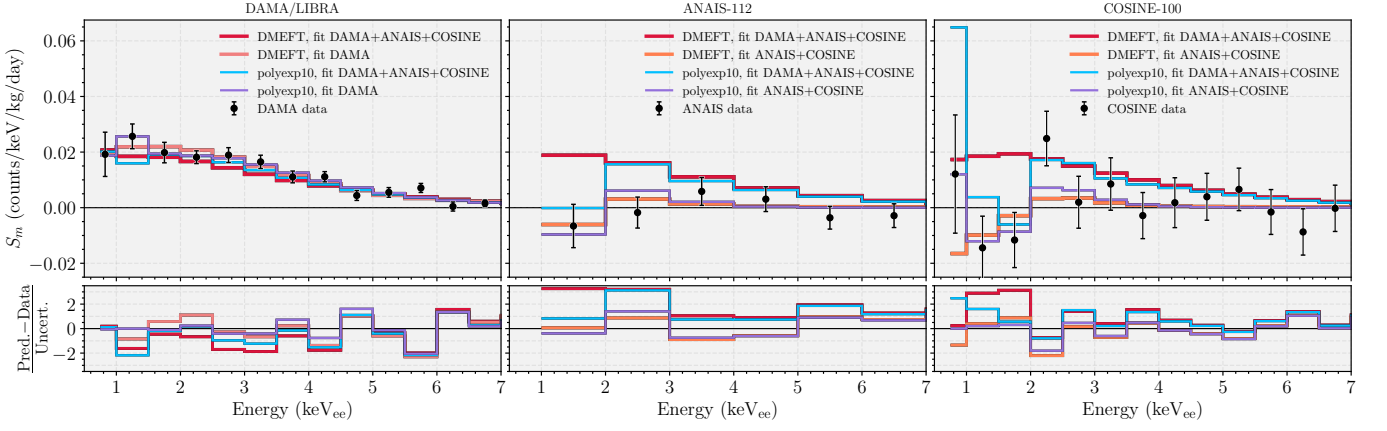


FIG. 1. Comparison of experimental data to the predicted rates at the best-fit points of selected fits.

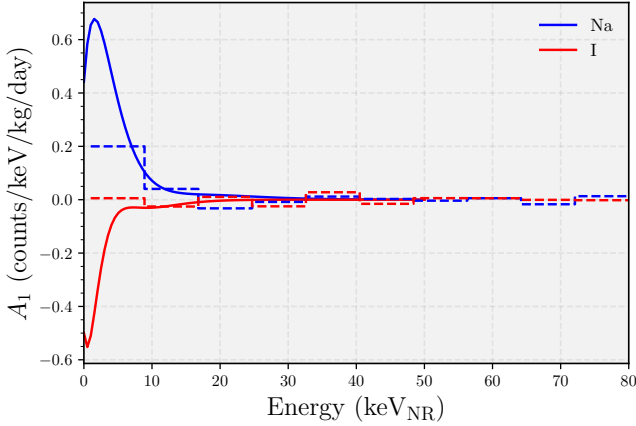


FIG. 2. Best-fit nuclear recoil spectra necessary to produce “only” a 3σ tension between DAMA/LIBRA and COSINE+ANAIS, using the polynomial-exponential parametrisation (15) (solid lines), and binned (2σ tension, dashed lines) with 10 times 2 bins. The pathological opposite-sign recoil between Na and I is generic of models that improve the overall fit.

thanks to their different binning, and therefore different mapping from nuclear to electronic recoil.

The DM-inspired parameterisation from Eq. (15) also leads to a reduced tension as the number of parameters is increased. When including only 4 free parameters (i.e. $c_0^T e^{-d_T E_R}$ for both sodium and iodine), the tension is above the 5σ level, but it drops modestly to 4.5, 4.1 and 3.2σ as linear, quadratic and cubic terms in energy are added, respectively.

As in the binned case, the best-fit points to the combined data tend to be pathological, preferring a signal with a positive modulation amplitude for Na, and negative for I. In other words, while recoils off sodium peak in the summer, nuclear recoils on iodine would need to peak in winter, or vice-versa. Fig. 1 shows the resulting signals in all three experiments in the case of the 10-parameter fit. The NR signal that leads to these results is in Fig. 2.

It is worth noting that this solution implies that the individual modulation amplitudes A_1^T in both sodium and iodine must be much larger than the actually observed modulation amplitude $A_1 = \sum_T A_1^T$. However, the positivity of the time-dependent event rate in Eq. (2) implies that the average rate A_0^T in each target must satisfy $A_0^T \gtrsim |A_1^T|$. If A_1^T has opposite sign for sodium and iodine, it follows that the total rate A_0 must be much larger than the observed modulation amplitude $|A_1|$. The total rate, on the other hand, can be constrained using independent measurements, such as the one presented by COSINE-100 in Ref. [19]. While our goal here is to remain as agnostic as possible about the total rates, this self-consistency requirement would place these scenarios under further strain.

Conclusion— We have revisited the tension between the DAMA/LIBRA, ANAIS-112 and COSINE-100 DM annual modulation datasets. For a Dirac fermion interacting with Standard Model particles through dimension-five and dimension-six operators, DAMA/LIBRA is in a 5.10σ tension with the other two experiments. This conclusion is now independent of the fact that direct search DM experiments with other target nuclei would exclude the DAMA/LIBRA excess. If instead a generic parameterisation of the modulation amplitude vs nuclear recoil energy is used, the tension is still greater than 5σ unless there is a significant degree of fine-tuning, resulting in a cancellation of the contributions from sodium and iodine. It remains interesting to consider a Southern hemisphere NaI experiment, such as the forthcoming SABRE South experiment [46], which may shed further light on the mystery, in particular because it is expected to place a world-leading limit on the total rate of DM scattering in NaI detectors.

ACKNOWLEDGMENTS

We thank Ankit Beniwal, Torsten Bringmann, Joachim Brod, Jan Conrad, Andrew Fowlie, Hyun Su Lee, Seung

Mok, Pat Scott, Sebastian Wild, Anthony Williams and Jure Zupan for useful input, along with the full GAMBIT collaboration. This work was performed using the Cambridge Service for Data Driven Discovery (CSD3), part of which is operated by the University of Cambridge Research Computing on behalf of the STFC DiRAC HPC Facility (www.dirac.ac.uk). The DiRAC component of CSD3 was funded by BEIS capital funding via STFC capital grants ST/P002307/1 and ST/R002452/1 and STFC operations grant ST/R00689X/1. DiRAC is part of the National e-Infrastructure. Additional support and computing resources from the Center for High Performance Computing at the University of Utah are gratefully acknowledged. GB is supported by the Australian Research Council grant CE200100008. JMC acknowledges support from the Weber State University College of Science and Academic Resources and Computing Committee. In addition, he is grateful to the Mainz Institute of

Theoretical Physics (MITP) of the Cluster of Excellence PRISMA⁺ (Project ID 39083149), for its hospitality and partial support during the completion of this work. FK acknowledges support from the DFG via Emmy Noether Grant No. KA 4662/1–2. AK is supported by the Research Council of Norway (RCN) through the FRIPRO grant 323985 PLUMBIN'. MP was supported by the Jim S. Bateman Research Fund at Weber State University. ACV was supported by Arthur B. McDonald Canadian Astroparticle Physics Research Institute, NSERC the Canada Foundation for Innovation and the Province of Ontario. Research at Perimeter Institute is supported by the Government of Canada through the Department of Innovation, Science, and Economic Development, and by the Province of Ontario. MJW is supported by the Australian Research Council grants CE200100008 and DP220100007.

-
- [1] R. Bernabei *et. al.*, *Dark matter search*, *Riv. Nuovo Cim.* **26N1** (2003) 1–73, [[astro-ph/0307403](https://arxiv.org/abs/astro-ph/0307403)].
 - [2] R. Bernabei *et. al.*, *Dark Matter: DAMA/LIBRA and its perspectives*, *SciPost Phys. Proc.* **12** (2023) 025, [[arXiv:2209.00882](https://arxiv.org/abs/2209.00882)].
 - [3] C. Kelso, P. Sandick, and C. Savage, *Lowering the Threshold in the DAMA Dark Matter Search*, *JCAP* **09** (2013) 022, [[arXiv:1306.1858](https://arxiv.org/abs/1306.1858)].
 - [4] S. Baum, K. Freese, and C. Kelso, *Dark Matter implications of DAMA/LIBRA-phase2 results*, *Phys. Lett. B* **789** (2019) 262–269, [[arXiv:1804.01231](https://arxiv.org/abs/1804.01231)].
 - [5] SuperCDMS Collaboration: R. Agnese, T. Aramaki, *et. al.*, *Results from the super cryogenic dark matter search experiment at soudan*, *Phys. Rev. Lett.* **120** (2018) 061802.
 - [6] R. Agnese, T. Aralis, *et. al.*, *First dark matter constraints from a supercdms single-charge sensitive detector*, *Phys. Rev. Lett.* **121** (2018) 051301.
 - [7] DarkSide Collaboration: P. Agnes, I. F. M. Albuquerque, *et. al.*, *Low-mass dark matter search with the darkside-50 experiment*, *Phys. Rev. Lett.* **121** (2018) 081307.
 - [8] PICO Collaboration: C. Amole, M. Ardid, *et. al.*, *Dark matter search results from the complete exposure of the pico-60 c₃f₈ bubble chamber*, *Phys. Rev. D* **100** (2019) 022001.
 - [9] LUX-ZEPLIN Collaboration: J. Aalbers, D. S. Akerib, *et. al.*, *First dark matter search results from the lux-zeplin (lz) experiment*, *Phys. Rev. Lett.* **131** (2023) 041002.
 - [10] XENON Collaboration: E. Aprile, K. Abe, *et. al.*, *First dark matter search with nuclear recoils from the xenonn1 experiment*, *Phys. Rev. Lett.* **131** (2023) 041003.
 - [11] B. Ahmed *et. al.*, *The NAIAD experiment for WIMP searches at Boulby mine and recent results*, *Astropart. Phys.* **19** (2003) 691–702, [[hep-ex/0301039](https://arxiv.org/abs/hep-ex/0301039)].
 - [12] S. C. Kim *et. al.*, *New Limits on Interactions between Weakly Interacting Massive Particles and Nucleons Obtained with CsI(Tl) Crystal Detectors*, *Phys. Rev. Lett.* **108** (2012) 181301, [[arXiv:1204.2646](https://arxiv.org/abs/1204.2646)].
 - [13] DM-Ice: E. Barbosa de Souza *et. al.*, *First search for a dark matter annual modulation signal with NaI(Tl) in the Southern Hemisphere by DM-Ice17*, *Phys. Rev. D* **95** (2017) 032006, [[arXiv:1602.05939](https://arxiv.org/abs/1602.05939)].
 - [14] J. Amaré *et. al.*, *First Results on Dark Matter Annual Modulation from the ANAIS-112 Experiment*, *Phys. Rev. Lett.* **123** (2019) 031301, [[arXiv:1903.03973](https://arxiv.org/abs/1903.03973)].
 - [15] J. Amare *et. al.*, *Annual modulation results from three-year exposure of ANAIS-112*, *Phys. Rev. D* **103** (2021) 102005, [[arXiv:2103.01175](https://arxiv.org/abs/2103.01175)].
 - [16] I. Coarasa *et. al.*, *ANAIS-112 three years data: a sensitive model independent negative test of the DAMA/LIBRA dark matter signal*, *Commun. Phys.* **7** (2024) 345, [[arXiv:2404.17348](https://arxiv.org/abs/2404.17348)].
 - [17] J. Amaré *et. al.*, *Towards a Robust Model-Independent Test of the DAMA/LIBRA Dark Matter Signal: ANAIS-112 Results with Six Years of Data*, *Phys. Rev. Lett.* **135** (2025) 051001, [[arXiv:2502.01542](https://arxiv.org/abs/2502.01542)].
 - [18] G. Adhikari *et. al.*, *An experiment to search for dark-matter interactions using sodium iodide detectors*, *Nature* **564** (2018) 83–86, [[arXiv:1906.01791](https://arxiv.org/abs/1906.01791)]. [Erratum: *Nature* 566, E2 (2019)].
 - [19] COSINE-100: G. Adhikari *et. al.*, *Strong constraints from COSINE-100 on the DAMA dark matter results using the same sodium iodide target*, *Sci. Adv.* **7** (2021) abk2699, [[arXiv:2104.03537](https://arxiv.org/abs/2104.03537)].
 - [20] COSINE-100: G. Adhikari *et. al.*, *Search for a Dark Matter-Induced Annual Modulation Signal in NaI(Tl) with the COSINE-100 Experiment*, *Phys. Rev. Lett.* **123** (2019) 031302, [[arXiv:1903.10098](https://arxiv.org/abs/1903.10098)].
 - [21] COSINE-100: G. Adhikari *et. al.*, *Three-year annual modulation search with COSINE-100*, *Phys. Rev. D* **106** (2022) 052005, [[arXiv:2111.08863](https://arxiv.org/abs/2111.08863)].
 - [22] N. Carlin *et. al.*, *COSINE-100 Full Dataset Challenges the Annual Modulation Signal of DAMA/LIBRA*, [[arXiv:2409.13226](https://arxiv.org/abs/2409.13226)].
 - [23] COSINE-100, ANAIS-112: N. Carlin *et. al.*, *Combined Annual Modulation Dark Matter Search with COSINE-100 and ANAIS-112*, [[arXiv:2503.19559](https://arxiv.org/abs/2503.19559)].
 - [24] R. Bernabei *et. al.*, *Further results from*

- DAMA/Libra-phase2 and perspectives*, *Nucl. Phys. Atom. Energy* **22** (2021) 329–342.
- [25] A. K. Drukier, K. Freese, and D. N. Spergel, *Detecting Cold Dark Matter Candidates*, *Phys. Rev. D* **33** (1986) 3495–3508.
- [26] D. N. Spergel, *The Motion of the Earth and the Detection of Wimps*, *Phys. Rev. D* **37** (1988) 1353.
- [27] K. Freese, J. A. Frieman, and A. Gould, *Signal Modulation in Cold Dark Matter Detection*, *Phys. Rev. D* **37** (1988) 3388–3405.
- [28] R. Bernabei *et. al.*, *Recent Results from DAMA/LIBRA and Comparisons*, *Moscow Univ. Phys. Bull.* **77** (2022) 291–300.
- [29] DAMA: R. Bernabei *et. al.*, *The DAMA/LIBRA apparatus*, *Nucl. Instrum. Meth. A* **592** (2008) 297–315, [[arXiv:0804.2738](#)].
- [30] S. Kang, S. Scopel, and G. Tomar, *Probing DAMA/LIBRA data in the full parameter space of WIMP effective models of inelastic scattering*, *Phys. Rev. D* **99** (2019) 103019, [[arXiv:1902.09121](#)].
- [31] J. Amaré *et. al.*, *Performance of ANAIS-112 experiment after the first year of data taking*, *Eur. Phys. J. C* **79** (2019) 228, [[arXiv:1812.01472](#)].
- [32] S. H. Lee *et. al.*, *Measurements of low-energy nuclear recoil quenching factors for Na and I recoils in the NaI(Tl) scintillator*, *Phys. Rev. C* **110** (2024) 014614, [[arXiv:2402.15122](#)].
- [33] M. Maltoni and T. Schwetz, *Testing the statistical compatibility of independent data sets*, *Phys. Rev. D* **68** (2003) 033020, [[hep-ph/0304176](#)].
- [34] M. J. Reid *et. al.*, *Trigonometric Parallaxes of High Mass Star Forming Regions: the Structure and Kinematics of the Milky Way*, *Astrophys. J.* **783** (2014) 130, [[arXiv:1401.5377](#)].
- [35] A. J. Deason, A. Fattahi, *et. al.*, *The local high-velocity tail and the galactic escape speed*, *MNRAS* **485** (2019) 3514–3526, [[arXiv:1901.02016](#)].
- [36] F. Bishara, J. Brod, B. Grinstein, and J. Zupan, *DirectDM: a tool for dark matter direct detection*, [[arXiv:1708.02678](#)].
- [37] J. Brod, A. Gootjes-Dreesbach, M. Tammaro, and J. Zupan, *Effective Field Theory for Dark Matter Direct Detection up to Dimension Seven*, *JHEP* **10** (2018) 065, [[arXiv:1710.10218](#)].
- [38] GAMBIT Collaboration: P. Athron, C. Balázs, *et. al.*, *GAMBIT: The Global and Modular Beyond-the-Standard-Model Inference Tool*, *Eur. Phys. J. C* **77** (2017) 784, [[arXiv:1705.07908](#)]. Addendum in [39].
- [39] GAMBIT Collaboration: P. Athron, C. Balázs, *et. al.*, *GAMBIT: The Global and Modular Beyond-the-Standard-Model Inference Tool. Addendum for GAMBIT 1.1: Mathematica backends, SUSYHD interface and updated likelihoods*, *Eur. Phys. J. C* **78** (2018) 98, [[arXiv:1705.07908](#)]. Addendum to [38].
- [40] GAMBIT Dark Matter Workgroup: T. Bringmann *et. al.*, *DarkBit: A GAMBIT module for computing dark matter observables and likelihoods*, *Eur. Phys. J. C* **77** (2017) 831, [[arXiv:1705.07920](#)].
- [41] GAMBIT Scanner Workgroup: G. D. Martinez, J. McKay, *et. al.*, *Comparison of statistical sampling methods with ScannerBit, the GAMBIT scanning module*, *Eur. Phys. J. C* **77** (2017) 761, [[arXiv:1705.07959](#)].
- [42] F. Bishara, J. Brod, B. Grinstein, and J. Zupan, *Chiral Effective Theory of Dark Matter Direct Detection*, *JCAP* **1702** (2017) 009, [[arXiv:1611.00368](#)].
- [43] F. Bishara, J. Brod, B. Grinstein, and J. Zupan, *From quarks to nucleons in dark matter direct detection*, *JHEP* **11** (2017) 059, [[arXiv:1707.06998](#)].
- [44] GAMBIT: P. Athron *et. al.*, *Global analyses of Higgs portal singlet dark matter models using GAMBIT*, *Eur. Phys. J. C* **79** (2019) 38, [[arXiv:1808.10465](#)].
- [45] R. Bernabei *et. al.*, *New limits on WIMP search with large-mass low-radioactivity NaI(Tl) set-up at Gran Sasso*, *Phys. Lett. B* **389** (1996) 757–766.
- [46] SABRE: E. Barberio *et. al.*, *Simulation and background characterisation of the SABRE South experiment: SABRE South Collaboration*, *Eur. Phys. J. C* **83** (2023) 878, [[arXiv:2205.13849](#)].

APPENDIX

We present additional details on the results of our fits in table III.

TABLE III. χ^2 values, p-values and tension statistics obtained by maximizing individual experimental likelihoods and the likelihood for all experiments combined for the generic functional form recoil spectra.

Model	Parameters	χ^2 : All	DAMA	COSINE+ANAIS	p-value	Tension (σ)
polyxexp (independent Na+I)	4	168.44	76.81	53.81	1.22×10^{-7}	5.16
	6	162.43	73.67	52.81	2.82×10^{-6}	4.54
	8	160.72	72.91	52.51	2.35×10^{-5}	4.07
	10	156.06	73.08	52.52	7.19×10^{-4}	3.19
Na only	2	181.91	92.33	57.76	1.23×10^{-7}	5.16
	3	168.10	76.90	57.60	2.41×10^{-7}	5.03
I only	2	188.31	86.25	57.83	2.49×10^{-10}	6.22
	3	177.83	75.81	57.81	1.36×10^{-9}	5.95
bins (independent Na + I)	2	204.77	103.65	58.02	4.36×10^{-10}	6.13
	4	194.57	75.94	56.54	1.05×10^{-12}	7.03
	6	176.70	74.02	51.30	2.49×10^{-9}	5.85
	10	159.90	59.66	45.60	3.69×10^{-8}	5.38
	12	156.98	56.99	44.74	1.63×10^{-7}	5.11
	16	139.75	52.38	39.54	5.07×10^{-5}	3.89
	20	121.59	46.60	40.52	2.31×10^{-2}	1.99
Na only	1	236.01	143.34	58.60	5.32×10^{-9}	5.72
	2	186.08	78.28	58.53	2.00×10^{-11}	6.60
	5	178.33	74.71	51.92	6.22×10^{-10}	6.07
	10	170.68	67.47	49.24	4.93×10^{-8}	5.33
I only	1	204.78	103.66	58.61	7.02×10^{-11}	6.42
	2	195.03	76.64	58.27	8.81×10^{-14}	7.37
	5	191.22	75.10	51.84	1.58×10^{-12}	6.97
	10	172.06	72.06	47.69	9.97×10^{-8}	5.20